STEEL FIBRE REINFORCED CONCRETE BEAMS – SIZE EFFECT

J. L. Vítek,
Department of Concrete Structures and Bridges, Faculty of Civil Engineering, Czech Technical University, Prague, and Metrostav, a.s., Prague, Czech Republic

Abstract

Experimental research of three sizes of large beams made of steel fibre reinforced concrete SFRC has been carried out at the CTU, Prague. The beams were subjected to four point bending. The ultimate load of the beams is proportional to their size, which means that no size effect has been observed at the ultimate load. The descending branch of the load deflection diagram is steeper at large beams than that at small beams. The large beams are more brittle, the descending branch is size dependent. A simple numerical model based on the discrete crack approach has been developed. Experimental and numerical results showed a good agreement.
Keywords: beam, concrete, energy, experiment, fibre, fracture, size effect

1 Experimental research

1.1 Scope of the experimental program

Fibre reinforced concrete became more popular in the last years. The technological as well as the mechanical issues are investigated. The aim

of our experimental program was to verify the production of larger elements and to contribute to better understanding of the performance and progressive failure of the beams subjected to bending. The extensive testing of small beams was arranged at the Czech Technical University in recent years, Vítek and Vítek (1995). However, the bigger size of specimens was necessary in order to get the results, which can be compared with those of actual structures. The beams of three sizes were subjected to the four point bending. The size effect on the failure load and on the post peak response was observed.

1.2 Concrete mix

A similar concrete mix like for reinforced concrete structures was used and the fibres were added before casting. The mix contains a course aggregate (32 mm) and relatively low amount of fibres (50 kg/m^3). The smooth steel fibres of the diameter 0.45 mm and 45 mm long were used. This amount of fibres is close to the workability limit. For the industrial use, it is recommended to add only 40 kg/m^3 of fibres. The composition of fibre reinforced concrete mix is shown in Table 1.

Table 1. Composition of FRC

	mm	kg/m^3
Sand	0 – 4	723
Crushed granite	4 - 8	181
	8 - 16	452
	16 - 32	452
Cement II (32.5 R)		320
Water		154
Plastisizer		2.5
Fibres	0.45/45	50

The compression strength tested on cubes (150 mm) was in the range 48 - 53 MPa. The splitting tensile strength measured on cubes varied from 4.0 to 5.0 MPa. The elastic modulus in compression measured on beams (150 x 150 x 700 mm) varied between 30.8 and 34.7 GPa.

1.3 Specimens

The smallest beams (series 1) were identical with the beams of the preceding series (span 600 mm). The second size (series 2) was 4 times larger and the third size (series 3) 8 times larger, however, the thickness of

beams was only 300 mm, so that the volume and weight of specimens were limited, and easier handling was possible. The weight of the largest beam was about 5 tons. The dimensions of the beams are shown in Table 2. Three beams were produced and tested in each series. Concrete was poured into the formwork and vibrated. The beams were kept in wet conditions in the formwork and after 7 days they were demoulded and left inside the laboratory in the room temperature (18°C).

Table 2. Dimensions of the specimens

	Depth [mm]	Width [mm]	Length [mm]	Span [mm]
Series 1	150	150	700	600
Series 2	600	300	2700	2400
Series 3	1200	300	5200	4800

1.4 Testing

The beams were loaded by two point loads symmetrically in the thirds of the span at the age of 31 days (small beams) and 35 days (medium and large beams). The loading process was controlled by the deflection at the midspan. The speed of loading was kept constant – 0.33 mm/min. The vertical displacements were measured at the midspan, under the point loads and at the supports. The gauges were placed on the both sides of beams and thus two readings at each point were obtained. Further gauges monitored the longitudinal strain in the central part of the beams. These gauges had rather long measuring length.

There were no notches on the beams. The crack appeared at all tested beams close to the midspan (as it was expected) and the longitudinal gauges measured the crack width. The gauges were also located at the top surface at the midspan in order to measure the strain in the compression zone.

The values obtained directly from readings could not be used for further evaluation. The measured load deflection curves had to be corrected by elimination of the two significant effects: (i) settlement of supports and (ii) effect of the dead load, which is important particularly at the largest beam size.

1.5 Results

A typical load deflection curves for the small and large beams are shown in Fig. 3a,b. The diagrams show the load-deflection curves after the corrections mentioned above. The amount of fibres is low and therefore the peak load is reached just before cracking. Then the load drops and the

fibres are activated if the crack opens. Due to the fibre action the load is kept on the level slightly over a half of the peak load, also at large deflections.

The relative comparison of the response of beams of different sizes is only possible using common relative values. Fig. 4 shows the comparison of the behaviour of all three sizes of specimens. The relative deflection is given by the ratio $w_R = w\, l_0/l$, where l_0 is a reference size. The nominal stress σ_N, as a relative value, is assumed as a ratio of a bending moment M and a section modulus W ($\sigma_N = M/W$). It can be seen that the ultimate (peak) stress is very similar at the specimens of all three sizes. There is observed no size effect at the peak load. However, it is possible to indicate that the large beam is more brittle than small beams, which means that the size effect may be seen at the descending branch of the load-deflection diagram.

2 Numerical modelling

2.1 Two phase material
Numerical models of cracking of quasi brittle materials are either smeared or discrete. In this case a discrete crack is assumed. The fibres crossing the crack carry a tensile force. The concrete matrix and the fibres – two phases - work together, forming a fibre reinforced concrete. This approach has been used already in Vítek and Vítek (1995). The new experimental results lead to necessary refinements.

The behaviour of concrete matrix is dependent on the reinforcement. The energy necessary for the crack progress in a plain concrete is not equal to that for crack progress in the matrix of fibre reinforced concrete. The difference may be explained on the element subjected to pure tension (Fig. 1). In cracked plain concrete the unloaded area is triangular. The elastic energy released due to unloading is consumed at least partly by the crack progress. In the case of FRC element, the fibres prevent a complete unloading of the triangle (Fig. 1a). A small part close to the crack tip is unloaded (corresponding to the crack length a_0), since the fibres are not activated and they do not transfer almost any tension. The rest of the crack ($a < a_1$, (Fig. 1b)) is not unloaded fully, fibres carry the tension. If a crack is long and more open, the fibres at the crack opening (a, (Fig. 1c)) do not carry any tension, they are already pulled out of concrete. The unloaded area is then of the triangular shape, similar to the plain concrete.

Plain concrete a)

SFRC - Initial stage b)

Unloaded area: ka
$A_0 = k\,a^2$

$A_0 = k\,a_0^2 + 2\,k a_0 a$

SFRC - Final stage c)

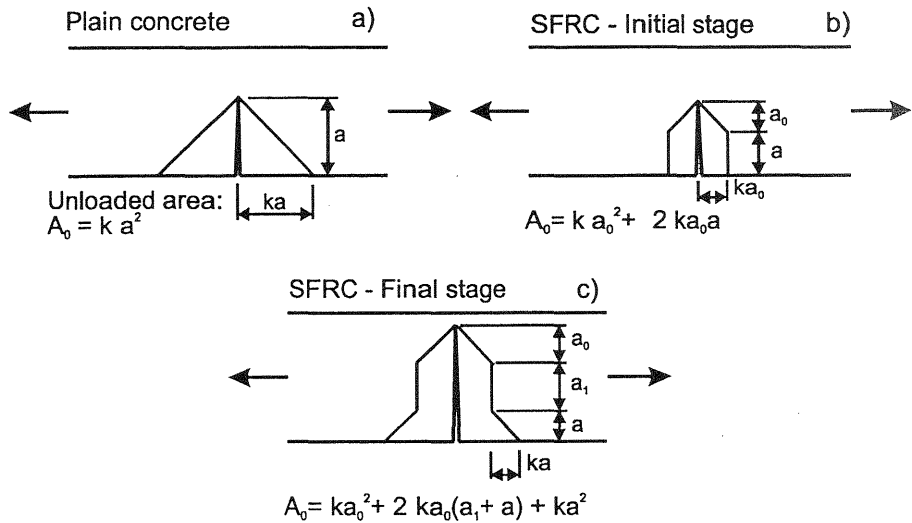$A_0 = k a_0^2 + 2\,k a_0 (a_1 + a) + k a^2$

Fig. 1. Fracture of the element subjected to tension

The energy released by unloading of a part of the element in the initial stage of the crack is similar at small and large elements. Unloaded area is linearly proportional to the crack length, $A_0 \sim a$ (Fig. 1b). In the final stage (large cracks), the unloaded area is dependent on a^2, ($A_0 \sim a^2$ (Fig. 1c)), similarly as it is in the case of plain concrete.

This example can help to explain the results of the experimental program, where the size effect was not observed at the peak load (initial stage of cracking). On the other hand it was observed at the descending branch (final stage of cracking).

A numerical model consists of the two parts – model of concrete matrix and model of fibres action. However, the fibres also influence the crack development in concrete matrix, as shown schematically in Fig. 1. The concrete interacts with fibres, which results in the compliance of concrete matrix, which is smaller than that of the plain concrete.

2.2 Simplified analysis based on LEFM
The stiffness of FRC beams is influenced preferably by the zone at the crack. If the crack is short the affected zone is larger, than that if the crack is large. In the limit case, if the crack length almost equals to the depth of the beam, this zone vanishes and the beam splits into two elastic elements.
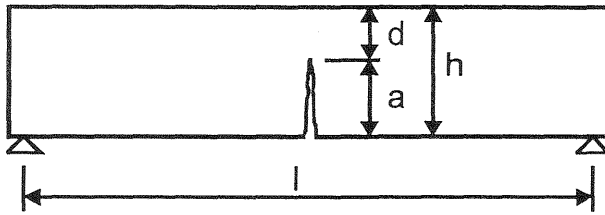
Fig. 2. Cracked beam - simplified method

It may be assumed, that the beam is composed of the three parts. Two parts (at the ends) are elastic and without any crack. The central part is also elastic, but its depth is reduced by the crack length a $(d = h\text{-}a)$ (Fig. 2). The length of the central part is considered to be also d. The load deflection diagram obtained using this simple model has been compared with the results of the finite element analysis of the beam with variable discrete crack and a very good agreement has been achieved.

The compliance of the beam can be expressed analytically. The load F (carried by the plain concrete) can be then determined according to linear fracture mechanics (LEFM)

$$F = \sqrt{\frac{2\,G_f\,b}{\dfrac{\partial C}{\partial a}}} \tag{1}$$

where b is a width of the beam, C is a compliance function of the beam and a is a crack length. In the case of the four point bending according to the simple model, it was assumed that

$$\frac{\partial C}{\partial a} = \left(\frac{l^2 - l\,d}{2h^3} + \frac{l^2}{d^3} + \frac{l}{4d^2}\right)/(E\,b) \tag{2}$$

where the dimensions are shown in Fig. 2.

The force carried by fibres is assumed in the form of an exponential function

$$F_1 = c_1 \exp(-c_2\,u) \tag{3}$$

where F_1 is a force in one fibre, c_1 and c_2 are constants, and u is a slip of the fibre, which is pulled off the concrete. The effect of variable orientation and position of fibres in concrete is taken into account by coefficients multiplying the number of fibres per unit area n.

As it was mentioned above, the compliance of FRC is lower than that of plain concrete (Eq. 2). The load carried by action of fibres is assumed to be F_f. The compliance, which reduces the compliance of plain concrete C, is then assumed as follows

$$C_f = \frac{F\,C}{F_f} \tag{4}$$

where C is a compliance of plain concrete. The compliance of the concrete matrix of FRC, C_{FM}, is dependent on the compliance of concrete and fibres

$$C_{FM} = \frac{1}{\dfrac{1}{C} + \dfrac{1}{C_f}} \tag{5}$$

The force carried by the matrix of FRC, F_{FM}, is given again according to the LEFM

$$F_{FM} = \sqrt{\frac{2\,G_f\,b}{\dfrac{\partial\,C_{FM}}{\partial\,a}}} \tag{6}$$

The total force carried by the cracked FRC beam F_{tot} is a sum of the force carried by the matrix and by fibres

$$F_{tot} = F_{FM} + F_f \tag{7}$$

2.3 Plastic limit
The equations above can be used for the analysis of load in dependence on the crack length. However, if the crack does not exist, the load carrying capacity is calculated according to the plastic limit analysis, which was described in Vítek and Vítek (1995).

However, due to the simplified modelling, $\partial\,C_{FM}/\partial a \neq 0$, at $a = 0$. This yields a peak on the load deflection curve. The ultimate load of the beam can be calculated in two ways: (i) by a plastic limit analysis or (ii) from Eq. 6, assuming the crack length $a = 0$. The lower value is taken as an ultimate load.
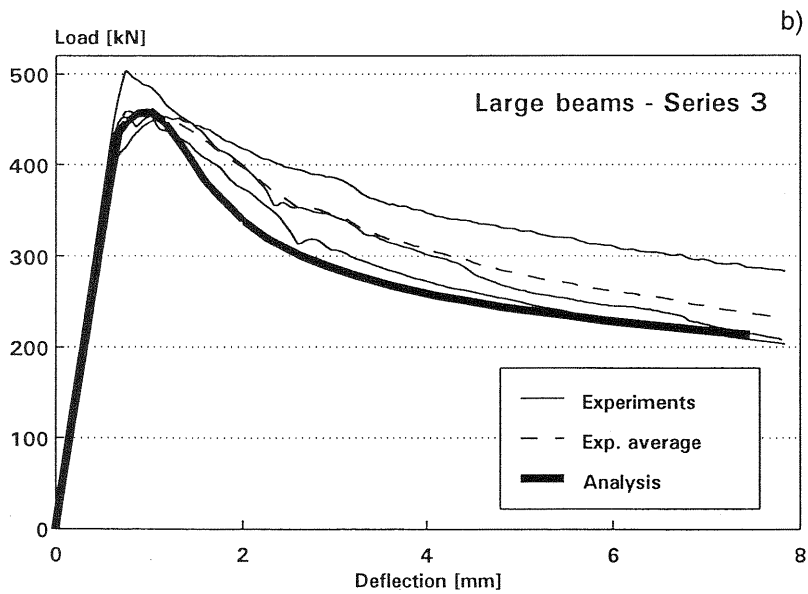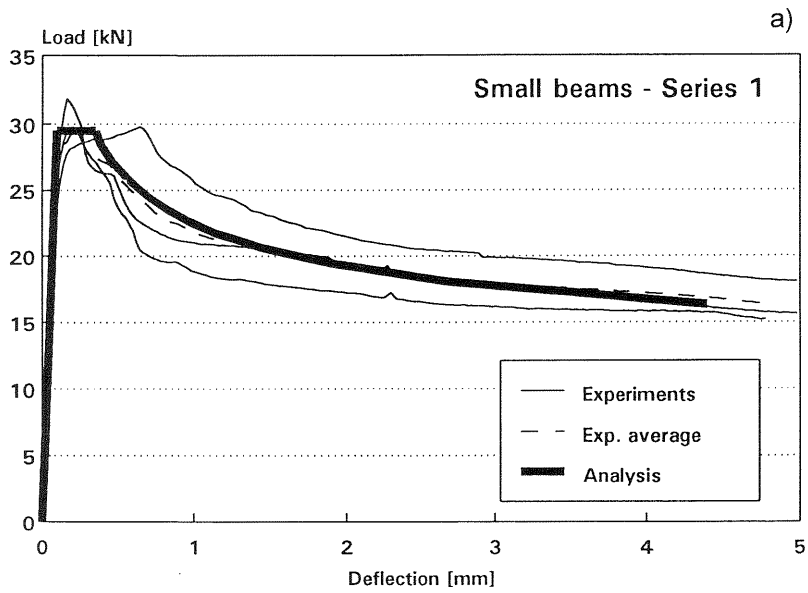
Fig. 3. Load deflection diagrams, experimental and calculated results.
a) Small beams, b) Large beams

3 Comparison of experimental and numerical results

The average values of the three tested specimens has been compared with the results of the simplified analysis. The load deflection diagrams of the small and large beams are shown in Figs. 3a and 3b. In the case of the small beams the peak load is limited by plastic limit analysis. In the case of the large beams the peak load is limited by Eq. 6.

The load deflection curves of beams of different sizes are plotted in Fig. 4, in terms of nominal stress versus relative deflection. The numerical model exhibits also no size effect at the peak load. The calculated descending branches are in a reasonable agreement with experimental curves.
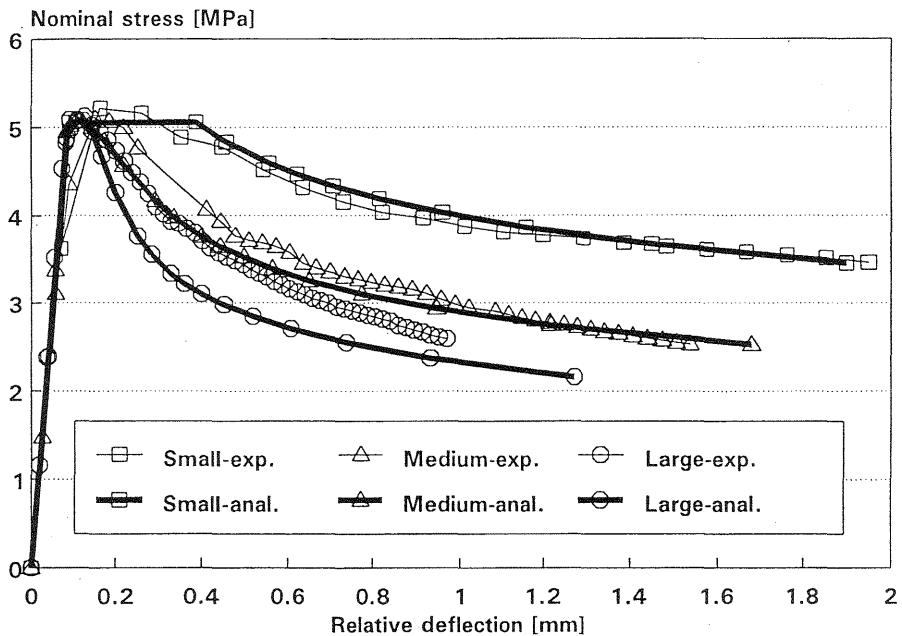
Fig. 4. Comparison of the response of beams of different sizes

4 Conclusions

- The concrete mix designed for the experiments may be used in industry. The fibres improve significantly the post peak resistance of the beams.
- The size effect on the peak load of the beams in the size range 1:8 was not observed experimentally.
- A simple numerical method based on the discrete crack has been developed and the absence of the size effect at the peak load has been confirmed also numerically.
- The descending branch of the load deflection diagram is dependent on the size of the beam. If the crack grows, the fibres come out of action, which results in more brittle behaviour of large beams.

References

Bažant, Z.P., Cedolin, L. (1991) **Stability of Structures: Elastic, Inelastic, Fracture and Damage Theories.** Oxford University Press, New York

Vítek, J.L., Vítek, P. (1995) Fracture of Fibre Reinforced Concrete Beams with Low Fibre Content in **Fracture Mechanics of Concrete Structures** (edt. F. H. Wittmann), AEDIFICATIO Publishers, Vol 1, Freiburg, 793-802